Frequency-dependent conductivity in bismuth-vanadate glassy semiconductors

Aswini Ghosh
Department of Solid State Physics, Indian Association for the Cultivation of Science, Jadavpur, Calcutta 700 032, West Bengal, India

(Received 26 September 1988; revised manuscript received 9 August 1989)

The first measurements are reported for the frequency-dependent (ac) conductivity (real as well as imaginary parts) for various compositions of the bismuth-vanadate glassy semiconductors in the frequency range 10^2-10^5 Hz and in the temperature range 77–420 K. The behavior of the ac conductivity is broadly similar to what has been observed previously in many other types of amorphous semiconductors, namely, nearly linear frequency dependence and weak temperature dependence. The experimental results are analyzed with reference to various theoretical models based on quantum-mechanical tunneling and classical hopping over barriers. The analysis shows that the temperature dependence of the ac conductivity is consistent with the simple quantum-mechanical tunneling model at low temperatures: however, this model completely fails to predict the observed temperature dependence of the frequency exponent. The overlapping-large-polaron tunneling model can explain the temperature dependence of the frequency exponent at low temperatures. Fitting of this model to the low-temperature data yields a reasonable value of the wave-function decay constant. However, this model predicts the temperature dependence of the ac conductivity much higher than what actual data showed. The correlated barrier hopping model is consistent with the temperature dependence of both the ac conductivity and its frequency exponent. This model provides reasonable values of the maximum barrier heights but higher values of characteristic relaxation times.

I. INTRODUCTION

Transition-metal oxide glasses have important semiconducting properties, which arise due to the presence of transition-metal ions in more than one valency state[1,2] [e.g., V^{5+} and V^{4+} in vanadate glasses]. The dc electrical conduction in these glassy semiconductors was observed to be due to the hopping of electrons or polarons from the ion of low-valency state to the ion of high-valency state of the transition metal.[1-5] It was also observed that at low frequencies and temperatures the frequency-dependent (ac) conductivity showed a nearly linear frequency dependence.[3,6,7] Some attempts[3,8-10] were made to study the low-frequency and low-temperature complex conductivity of the transition-metal oxide glassy semiconductors with the help of various theoretical models proposed for the ac conduction in amorphous semiconductors.

The objective of the present work is to study the frequency and temperature dependence of the ac conductivity of various compositions of the bismuth-vanadate glassy semiconductors over the frequency $(\omega/2\pi)$ range 10^2-10^5 Hz and the temperature range 77–420 K. In Sec. II various theoretical models proposed for the ac conduction in amorphous semiconductors are briefly described. Section III concerns the experimental procedure. The results are presented in Sec. IV and are analyzed in Sec. V with the help of models described in Sec. II.

II. THEORETICAL MODELS

The total conductivity $\sigma_{\rm tot}(\omega)$ measured in a given experiment at particular frequency ω and temperature can be written as

$$\sigma_{\rm tot}(\omega)=\sigma(\omega)+\sigma_{\rm dc} \tag{1}$$

where $\sigma_{\rm dc}$ and $\sigma(\omega)$ are the dc and frequency-dependent (ac) conductivities, respectively, and it is tacitly assumed that the ac and dc conductivities are due to completely different processes. When the ac and dc conductivities arise due to the same process and $\sigma_{\rm dc}$ is simply $\sigma(\omega)$ in the limit $\omega\rightarrow 0$, then the separation given in Eq. (1) is no longer useful.

In many amorphous semiconductors and insulators,[11] the ac conductivity invariably has the form

$$\sigma(\omega)=A\omega^{s}\ , \tag{2}$$

where A is a constant dependent on temperature and the exponent s is generally less than or equal to unity. All that is required to give this behavior is that the loss mechanism should have a very wide range of possible relaxation times, τ. In particular, a nearly linear frequency dependence of $\sigma(\omega)$ is predicted if the distribution of relaxation times $n(\tau)$ is inversely proportional to τ, which results if $\tau=\tau_0\exp(\zeta)$ where ζ is a random variable and τ_0 a characteristic relaxation time often taken to be an inverse phonon frequency, $\nu_{\rm ph}^{-1}$. Any departures from linearity carry information on the particular type of loss mechanism involved.

Many different theories[12,13] for ac conduction in amorphous semiconductors have been proposed. It is commonly assumed that the pair approximation holds, namely, the dielectric loss occurs because the carrier motion is considered to be localized within pairs of sites. This is the high-frequency limit of the general case where multi-

ple hopping can occur between a number of centers in a cluster. In essence, two distinct processes have been proposed for the relaxation mechanism, namely, quantum-mechanical tunneling and classical hopping over a barrier, or some combination or variant of the two, and it has been variously assumed that electrons (or polarons) or atoms are the carriers responsible.

To compare the various models with the experimental data, the detailed predictions of the temperature and frequency dependence of the ac conductivity need to be examined and thus each approach is discussed below in brief.

For the quantum-mechanical tunneling (QMT) model, the random variable is $\zeta=2\alpha R$, where R is the intersite separation and α^{-1} is the spatial decay parameter for the s-like wave function assumed to describe the localized state at each site and it is commonly assumed that α is a constant for all sites. Several authors[2,13–17] have evaluated, within the pair approximation, the ac conductivity for single-electron motion undergoing QMT and obtained the following expression:

$$\sigma(\omega)=Ce^2k_BT\alpha^{-1}[N(E_F)]^2\omega R_\omega^4 , \tag{3}$$

where C is a numerical constant which varies slightly according to different authors, but may be taken as $\pi^4/24$ (Refs. 13, 15, and 17). $N(E_F)$ is the density of states at the Fermi level (assumed constant) and R_ω is the hopping distance at a particular frequency ω, given by

$$R_\omega=\frac{1}{2\alpha}\ln(1/\omega\tau_0) . \tag{4}$$

The frequency dependence of $\sigma(\omega)$ in the form of Eq. (2) can be deduced using the relation

$$s=\frac{d\ln\sigma(\omega)}{d\ln\omega} \tag{5}$$

and for the QMT model [Eq. (3)], this gives

$$s=1-\frac{4}{\ln(1/\omega\tau_0)} . \tag{6}$$

The above results are obtained in a wide-band case, i.e., for $\Delta_0\gg k_BT$, where Δ_0 is the bandwidth. Thus for the QMT model, the frequency exponent s is temperature independent but frequency dependent, and for typical values of the parameters, namely, $\tau_0\simeq10^{-13}$ s and $\omega=10^4$ s^{-1}, a value of $s=0.81$ is deduced from Eq. (6).

A temperature-dependent frequency exponent can be obtained within the framework of the QMT model in the pair approximation by assuming that the carriers form nonoverlapping small polarons,[11] i.e., the total energy of a charge carrier is lowered by the polaron energy W_p resulting from the lattice distortion accompanying the occupation of a site by a carrier. Transport of an electron between degenerate sites having a random distribution of separations will, therefore, generally involve an activation energy, the polaron hopping energy $W_H\simeq W_P/2$. In this case, the frequency exponent becomes

$$s=1-\frac{4}{\ln(1/\omega\tau_0)-W_H/k_BT} . \tag{7}$$

Now it is noted that s is temperature dependent, increasing with increasing temperature. It should also be noted that a temperature-dependent frequency exponent can arise from the simple QMT model if pair approximation breaks down, i.e., when the carrier motion occurs within clusters.[18] The tunneling distance at a frequency ω in the nonoverlapping-small-polaron model becomes

$$R_\omega=\frac{1}{2\alpha}[\ln(1/\omega\tau_0)-W_H/k_BT] \tag{8}$$

and the ac conductivity is given by Eq. (3), but with the above expression for R_ω. The behavior of this model might, at first sight, appear to be pathological in that s can apparently become infinity at sufficiently high frequency and/or low temperatures due to the hopping length R_ω tending to zero, when the term in the square brackets in the above expression [Eq. (8)] for R_ω tends to zero. In practice, of course, the minimum value of R_ω is equal to the interatomic spacing; for higher frequencies or lower temperatures than given by the critical conditions, the contribution to the overall ac conductivity due to the small-polaron tunneling mechanism would tend to zero.

Long[13] has proposed a mechanism for the polaron tunneling model where the large polaron wells of two sites overlap, thereby reducing the value of polaron hopping energy,[2,18] i.e.,

$$W_H=W_{H0}(1-r_p/R) , \tag{9a}$$

where r_p is the polaron radius and W_{H0} is given by

$$W_{H0}=\frac{e^2}{4\epsilon_p r_p} \tag{9b}$$

where ϵ_p is the effective dielectric constant. It is assumed once again that W_{H0} is constant for all sites, whereas the intersite separation R is a random variable. The ac conductivity for the overlapping-large-polaron tunneling (OLPT) model[13] is given by

$$\sigma(\omega)=\frac{\pi^4}{12}e^2(k_BT)^2[N(E_F)]^2\frac{\omega R_\omega^4}{2\alpha k_BT+W_{H0}r_p/R_\omega^2} , \tag{10}$$

where R_ω is the hopping length at a frequency ω determined by the quadratic equation

$$(R'_\omega)^2+[\beta W_{H0}+\ln(\omega\tau_0)]R'_\omega-\beta W_{H0}r'_p=0 , \tag{11}$$

where $R'_\omega=2\alpha R_\omega$, $r'_p=2\alpha r_p$, and $\beta=1/k_BT$. The frequency exponent s of $\sigma(\omega)$ in this model can be evaluated as

$$s=1-\frac{8\alpha R_\omega+6\beta W_{H0}r_p/R_\omega}{(2\alpha R_\omega+\beta W_{H0}r_p/R_\omega)^2} . \tag{12}$$

Thus the OLPT model predicts that s should be both temperature and frequency dependent. It can also be seen from Eq. (12) that s decreases from unity with increasing temperature. For large values of r'_p, s continues to decrease with increasing temperature, eventually tending to the value of s predicted by the QMT model of non-

polaron forming carriers, whereas for small values of r_p', s exhibits a minimum[13] at a certain temperature and subsequently increases with increasing temperature in a similar fashion to the case of small-polaron QMT.

The other type of process, which has been proposed for the relaxation mechanism, is classical hopping over a barrier (HOB), where the random variable is $\zeta = W/k_B T$. For the case of atomic motion the following expression is obtained[13,19] for ac conductivity:

$$\sigma(\omega) = \frac{\pi}{3}\eta \frac{Np^2 k_B T}{W_0 \Delta_0}\omega \tanh(\Delta_0/2k_B T) , \tag{13}$$

where η is a mean-field correction term, N is the number of pair states per unit volume, p is the dipole moment associated with the transition, and it is assumed that the energy difference between sites, Δ, is randomly distributed in the range $0 < \Delta < \Delta_0$ and the barrier height is also randomly distributed in the range $0 < W < W_0$. It is noted from Eq. (13) that for this simple HOB model, the frequency exponent of $\sigma(\omega)$ is predicted to be unity and is independent of temperature and frequency. It might be mentioned here that even for the case of atomic tunneling, an expression similar to Eq. (13) for $\sigma(\omega)$ is obtained,[20] again with $s = 1$, if the dipole moment is uncorrelated with the tunneling distance.[13]

A model for ac conduction, which correlates the relaxation variable W with the intersite separation R, has been developed initially by Pike[21] for single-electron hopping and extended by Elliott[12,22] for two electrons hopping simultaneously. For neighboring sites at a separation R, the Coulomb wells overlap, resulting in a lowering of the effective barrier from W_M to a value W, which for the case of two-electron transition is given by[12]

$$W = W_M - \frac{2e^2}{\pi\epsilon\epsilon_0 R} , \tag{14}$$

where ϵ is the dielectric constant of the material and ϵ_0 that of free space. The ac conductivity in this model, termed the correlated barrier hopping (CBH) model,[23] in the narrow-band limit ($\Delta_0 \ll k_B T$) is expresed by

$$\sigma(\omega) = \frac{\pi^3}{12} N^2 \epsilon\epsilon_0 \omega R_\omega^6 , \tag{15}$$

where N is the concentration of pair sites and R_ω is the hopping distance given by

$$R_\omega = \frac{2e^2}{\pi\epsilon\epsilon_0 [W_M + k_B T \ln(\omega\tau_0)]} . \tag{16}$$

The frequency exponent s for this model is evaluated as[12]

$$s = 1 - \frac{6k_B T}{W_M + k_B T \ln(\omega\tau_0)} , \tag{17}$$

which to a first approximation reduces to the simple expression

$$s = 1 - 6k_B T / W_M . \tag{18}$$

Thus, in the CBH model a temperature-dependent exponent is predicted, with s increasing towards unity as $T \to 0$ K, in marked contrast to the QMT or simple HOB mechanism. In the broadband, i.e., low-temperature limit ($\Delta_0 \gg k_B T$), N in the expression (15) is replaced by $Nk_B T/2\Delta_0$ and so an additional T^2 dependence of $\sigma(\omega)$ is introduced.[13] It should be mentioned that for the single-electron CBH model the expressions (15) and (16) are multiplied by $\frac{1}{2}$ and the expression (17), however, remains unaltered.

It might appear that the behavior of the CBH model is also pathological in the same sense as discussed previously for the small-polaron QMT model. In this case, however, when the denominator of Eq. (16) tends to zero, R_ω tends to infinity. However, long before this can occur, the pair approximation breaks down, and the dc percolation limit is reached with the result that the CBH model is no longer valid.[12]

Several developments of this theory have been made. The assumption of randomly distributed centers used in the derivation of Eq. (15) has been relaxed for the case of melt-quenched chalcogenide glasses where pairing of charged defects may occur. The result of this is an enhancement of the frequent exponent s [Eq. (17)] by an additional factor $T/8T_g$ where T_g is the glass transition temperature.[24]

III. EXPERIMENTAL PROCEDURE

The samples were prepared from analar-grade V_2O_5 (Reanal, Hungary) and Bi_2O_3 (E. Merck, Germany). A proportionate mixture (Table I) of these chemicals was melted in an alumina crucible.

The melt was held at 900 °C in an electrical furnace for two hours and was shaken frequently to ensure proper

TABLE I. Final glass compositions and some physical parameters of the bismuth-vanadate glassy semiconductor.

Glass composition (mol %)		Density	$[V^{5+}]+[V^{4+}]$	$[V^{4+}]$	R	s
V_2O_5	Bi_2O_3	(g cm^{-3})	(cm^{-3})	(cm^{-3})	(Å)	at 80 K
70.8	29.2	3.49	2.05×10^{22}	7.69×10^{20}	3.65	0.93
75.6	24.4	3.40	2.12×10^{22}	4.50×10^{20}	3.61	0.92
80.5	19.5	3.32	2.20×10^{22}	4.21×10^{20}	3.57	0.90
85.5	14.5	3.26	2.25×10^{22}	4.00×10^{20}	3.54	0.88
90.3	9.7	3.17	2.28×10^{22}	3.96×10^{20}	3.52	0.87
95.2	4.8	3.02	2.34×10^{22}	3.75×10^{20}	3.49	0.85

mixing and homogeneity. The melt was then poured onto an ice-cooled stainless-steel block and was pressed immediately by a similar stainless-steel block. Quite stable and homogeneous samples of thickness 0.5–1.0 mm with glassy appearance were obtained.

The amorphous nature of the samples (as prepared as well as annealed at 200 °C for 2 hs) was confirmed by x-ray diffraction (Phillips, model PW 1050/1051) and scanning electron microscopy (Hitachi, model S-415A) studies.

For electrical measurements, disk-shaped samples of diameter ~8–10 mm were cut and polished with very fine lapping papers. The ac measurements were carried out in a General Radio (model GR-1615A) capacitance bridge which measures equivalent parallel conductance and capacitance of a sample for frequencies ($\omega/2\pi$) between 20 and 10^5 Hz in a three-terminal arrangement, using gold as electrode material. An evacuable chamber was employed as a sample cell and was inserted inside a cryostat for low-temperature measurements. Measurements were made in the temperature range 77–420 K with a stability of ±0.5 K.

The final composition of the samples and the concentrations of total vanadium ions were determined by a redox-titration method.[5] The concentrations of the reduced V^{4+} ions were estimated from EPR spectra obtained using a Varian E-12 *X*-band spectrometer. A single crystal of copper sulphate pentahydrate was used as a standard. The density of the samples was determined by a displacement method. The average intersite separation (R) (Table I) was obtained from the final composition and density.

IV. RESULTS

Figure 1 shows the measured total conductivity $\sigma_{tot}(\omega)$ and also the dc conductivity σ_{dc} as a function of reciprocal temperature at various frequencies for one glass composition (as prepared and annealed). From this figure it is observed that, in common with other amorphous semiconductors, the temperature dependence of $\sigma_{tot}(\omega)$ is much less than that of σ_{dc} at low temperatures, and is not activated in behavior. However, at high temperatures the temperature dependence of $\sigma_{tot}(\omega)$ becomes strong and its frequency dependence becomes small. Ultimately, the measured conductivities at all frequencies coincide with σ_{dc} at higher temperatures. Similar behaviors were also observed for other glass compositions, the only difference existing in the temperature at which the measured conductivity becomes equal to the dc conductivity. It is also observed from Fig. 1 that the effect of annealing on the conductivity is not significant for the present vanadate glassy semiconductor.

The measured conductivity as a function of frequency at various temperatures is shown in Fig. 2(a) for the same glass composition as shown in Fig. 1. It is also evident from this figure that the dc contribution is significant at low frequencies and high temperatures, while the frequency-dependent term dominates at high frequencies and low temperatures. Figure 2(b) shows the frequency dependent (ac) conductivity $\sigma(\omega)$ (real part), obtained by subtracting the dc conductivity from the measured conductivity, as a function of frequency at the same temperature and for the same glass composition as in Fig. 2(a). The solid lines in Fig. 2(b) are the straight-line fit obtained by the least-squares fitting procedure. The frequency exponent s was computed from the slope of the solid lines. In the investigated frequency range, frequency dependence of s was not observed, even at high temperatures. Figure 3 depicts the frequency dependence of the ac conductivity at 80 K for various glass compositions. The frequency exponent s at 80 K, obtained by the above fitting procedure, is shown in Table I, from which it is observed that the frequency exponent decreases with

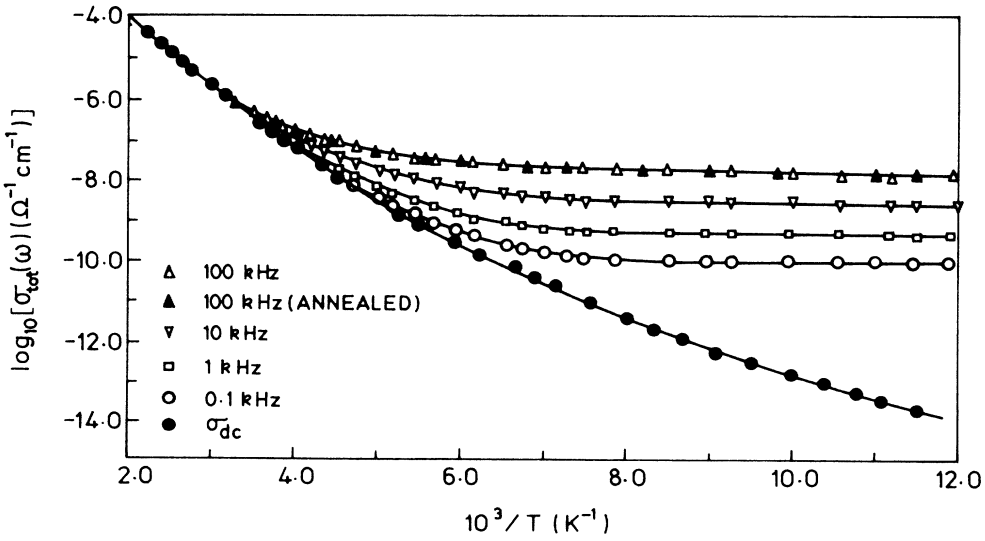

FIG. 1. Measured total conductivity for the sample composition $80(V_2O_5)$-$20(Bi_2O_3)$ shown as a function of inverse temperature at four frequencies shown. The measured dc conductivity is also shown (Ref. 5). The effect of annealing at 200 °C for 2 h is shown for one frequency.

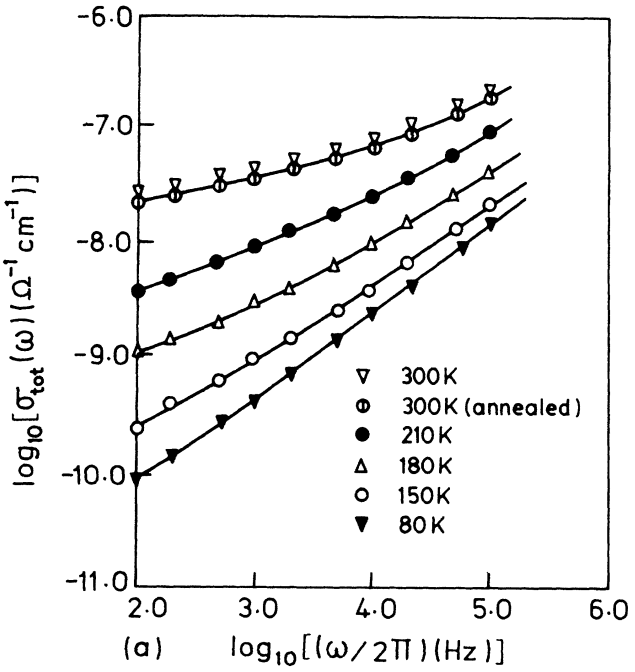

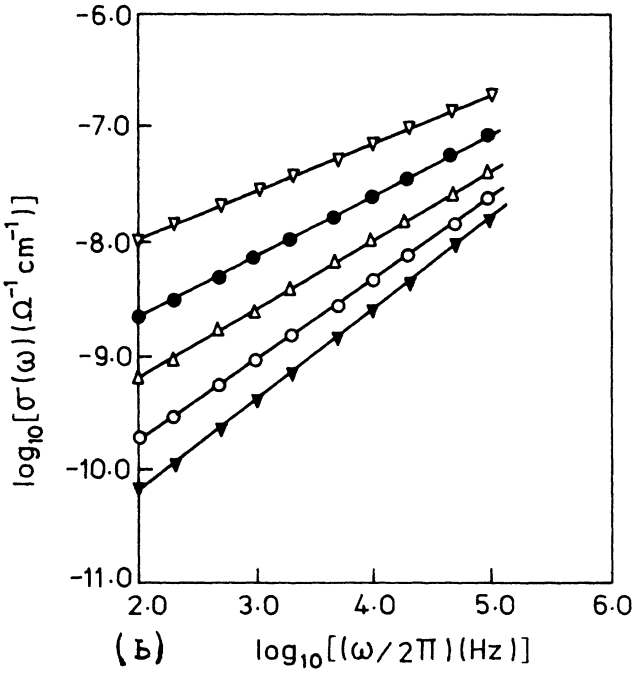

FIG. 2. (a) Frequency dependence of the measured total conductivity for the sample composition $80(V_2O_5)$-$20(Bi_2O_3)$ at several temperatures shown. The solid curves in this figure are the fits made using the ac conductivity calculated from the CBH model [Eq. (15)] and the measured value of the dc conductivity σ_{dc}. (b) The frequency-dependent conductivity obtained by subtracting the dc conductivity from the data shown in (a). The solid lines are the straight-line fits obtained by a least-squares fitting procedure.

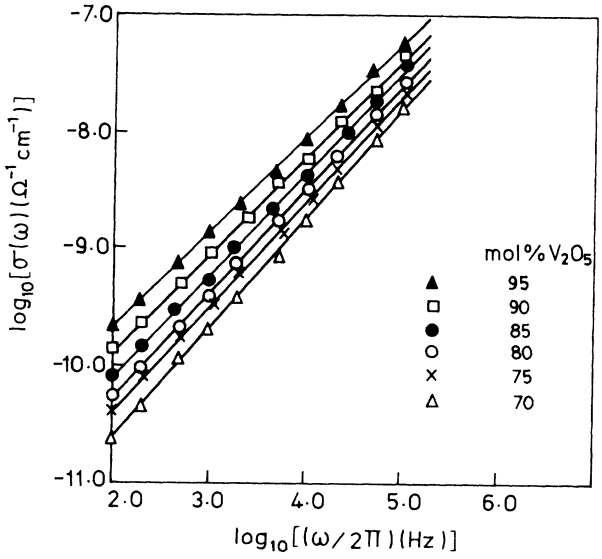

FIG. 3. The frequency-dependent conductivity, obtained by subtracting the dc conductivity from the measured total conductivity, at a fixed temperature (80 K) for the various glass compositions, shown as a function of frequency. The solid lines are the straight-line fits obtained by the least-squares fitting procedure as in Fig. 2(b).

the increase of V_2O_5 content in the glass. Figure 4 shows the temperature dependence of the frequency exponent s for one glass composition. From this figure it is observed that the frequency exponent decreases smoothly with increasing temperature. Other glass compositions also showed similar behaviors.

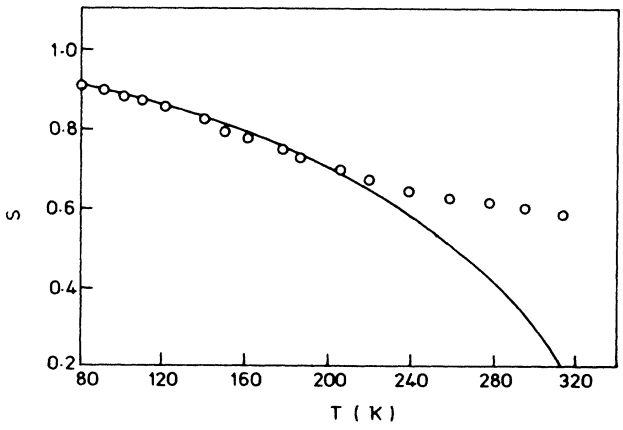

FIG. 4. Temperature dependence of the frequency exponent s for the sample composition $80(V_2O_5)$-$20(Bi_2O_3)$, obtained by the fitting procedure as in Figs. 2(b) and 3. The solid curve in the figure is calculated using the CBH model [Eq. (17)], with the parameters given in Table IV, assuming a fixed frequency $\omega = 10^4\ s^{-1}$.

V. DISCUSSIONS

A. Quantum-mechanical tunneling model

The mechanism of quantum-mechanical tunneling has previously been applied to ac conductivity data for many amorphous semiconductors without conspicuous success and it turns out that the behavior of the present glass system cannot be reconciled with this theory. Perhaps, the most obvious discrepancy between experiment and theory concerns the frequency dependence of s, the frequency exponent of the ac conductivity. The QMT model [Eq. (6)] predicts, in its simplest form, a value for $s \sim 0.81$, independent of temperature. However, it can be clearly seen from Fig. 4 that the general trend for s is to decrease with increasing temperature, thereby conflicting with the prediction of the simple QMT model. For the QMT model of the nonoverlapping small polaron, a temperature dependence of s is predicted, but it is of opposite sign [Eq. (7)]. The simple QMT model also predicts that s should decrease appreciably with increasing frequency.[12] No such variation was observed for the present glass system in the investigated frequency range (10^2–10^5 Hz).

Nevertheless, Eq. (3) suggests the temperature dependence of the ac conductivity in the form $\sigma(\omega) \propto T^n$ with $n=1$. From the plot of $\log_{10}\sigma(\omega)$ versus $\log_{10}T$ (Fig. 5) for the vanadate glass, it is observed that the ac conductivity increases linearly with temperature [i.e., $\sigma(\omega) \propto T^n$ with $n=1$] over a considerable range of low temperature (below 200 K). However, at higher temperatures the ac conductivity starts to deviate from linearity, and the temperature at which deviation from linearity starts, increases with increasing frequency.

Fits to the experimental values of $\sigma(\omega)$ made using Eq. (3) as a function of temperature are shown in Fig. 5. The values of parameters used are shown in Table II. In the fitting procedure, a fixed value of the decay constant (~ 1.0 Å^{-1}) and a fixed frequency ($\omega/2\pi = 10^4$ Hz) were assumed. The values of τ_0, obtained in the fitting procedure, are larger by one order than the inverse phonon frequency $\nu_{\rm ph}^{-1}$ estimated from other experiments.[5] Several authors[11,22] have pointed out the uncertainty in the values of $N(E_F)$ from the ac data and it is believed that the ac data usually give a higher value of $N(E_F)$ than that estimated by other techniques such as optical absorption or photoinduced ESR.[22]

B. Overlapping-large-polaron tunneling model

The overlapping-large-polaron tunneling model predicts that $\sigma(\omega)$ should have a negative temperature dependence of s at least at low temperatures [cf. Eq. (12)]. Thus at first sight, it appears that the OLPT model might be a possible candidate theory to explain the data presented here. In order to verify this, the frequency exponent s is plotted as a function of $k_B T/W_{H0}$ in Fig. 6. The theoretical curves given by Eq. (12) are also drawn in Fig. 6 for various values of the normalized polaron radius r_p'. The best fit to the experimental points has been observed for the values of W_{H0} shown in Table III. As seen from Fig. 6, the experimental values of s reside between the theoretical curves for $r_p' = 1.4$ to 3.0 at low temperatures.

TABLE II. Parameters for various glass compositions, obtained by fitting low-temperature ac data to the QMT model.

Glass composition mol% V_2O_5	τ_0 (s)	$N(E_F)$ ($eV^{-1}cm^{-3}$)
70.8	6.3×10^{-12}	7.60×10^{20}
75.6	7.5×10^{-12}	9.75×10^{20}
80.5	9.0×10^{-12}	1.56×10^{21}
85.5	2.1×10^{-11}	1.71×10^{21}
90.3	3.6×10^{-11}	1.81×10^{21}
95.2	6.8×10^{-11}	2.18×10^{21}

The polaron radius r_p can be calculated from Eq. (9a) from the known values of the average intersite separation R and polaron hopping energy W_H. The polaron hopping energy may be assumed approximately equal to the high-temperature activation energy W (Table III) for dc conduction.[5] Knowing r_p, the decay constant can also be estimated from the relation $r_p' = 2\alpha r_p$. The estimated values of α (shown in Table III) are in good agreement with the values obtained from the analyses of the dc conductivity data.[5,25] But the estimated values of r_p (Table III) is smaller than the vanadium site spacing R (Table I), which appears to be inconsistent with the basic premise of overlapping polarons.

However, at higher temperatures the experimental points do not lie between the theoretical curves and it has been observed that the decrease of s with increasing temperature is higher than what is predicted by the OLPT model.

The OLPT model [Eq. (10)] also predicts the frequency

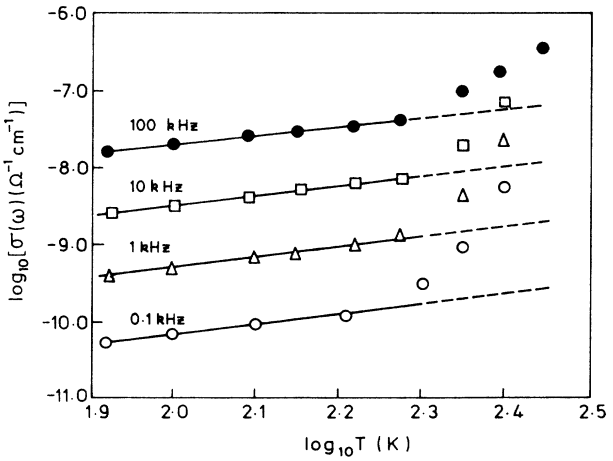

FIG. 5. Temperature dependence of the frequency-dependent conductivity, obtained by the subtraction procedure as in Figs. 2(b) and 3, for the sample composition $80(V_2O_5)$-$20(Bi_2O_3)$, plotted double logarithmically. The solid lines are the fits made using the QMT model [Eq. (3)].

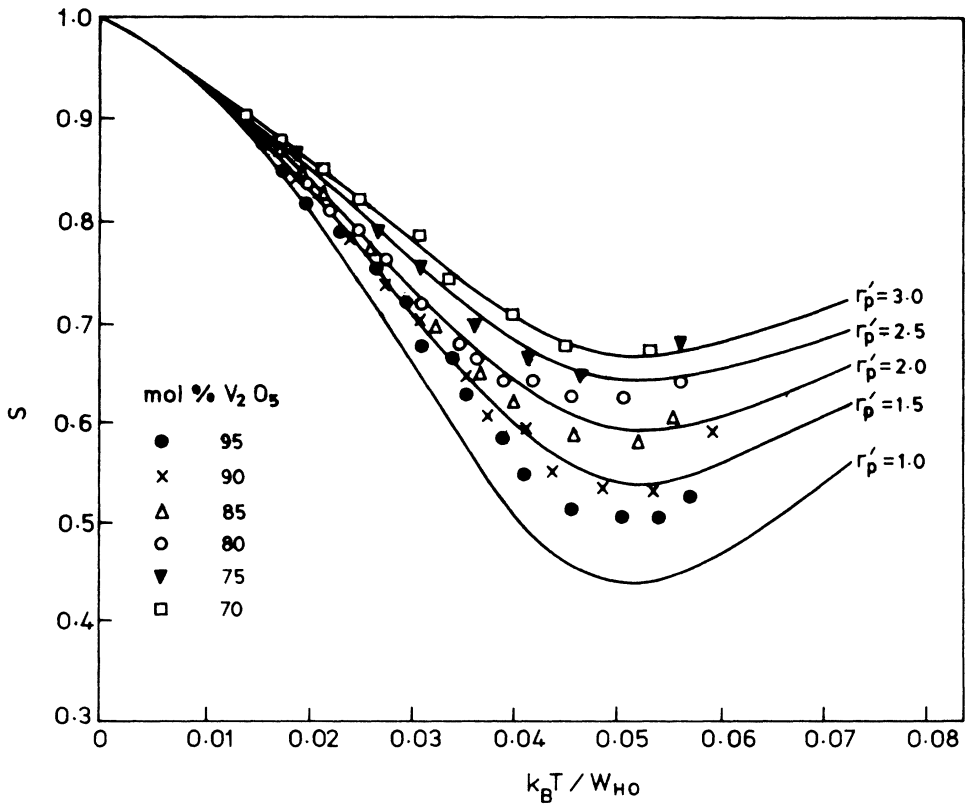

FIG. 6. The frequency exponent s for various glass compositions shown as a function of k_BT/W_{H0}. The solid curves are calculated from the OLPT model [Eq. (12)] for a fixed value of $\ln(\omega\tau_0)=-20$ and for various values of the normalized polaron radius r_p' shown.

dependence of s. A detailed analysis shows that in the low-temperature region ($k_BT/W_{H0}<0.04-0.05$) s should increase with frequency. The effect is small at low temperatures. For example, for $k_BT/W_{H0}=0.01-0.05$, $\Delta s\simeq 0.01-0.05$ when frequency changes by six orders of magnitude. An opposite and more significant behavior should be observed in the high-temperature region ($k_BT/W_{H0}>0.05$) where s changes with frequency. In the present experiment, the change in frequency did not exceed three orders of magnitude and the frequency dependence of s was not observed.

Regarding the temperature dependence of $\sigma(\omega)$: the OLPT model predicts a considerably stronger temperature dependence in the temeprature regime where the frequency exponent s is a decreasing function of temperature. The functional form of the temperature dependence of $\sigma(\omega)$ predicted by the OLPT model [Eq. (10)] is complicated and cannot be expressed simply as $\sigma(\omega)\propto T^n$ with n constant over a wide temperature range. Nevertheless, at low temperatures ($k_BT/W_{H0}<0.04-0.05$) the hopping length R_ω has an approximately constant temperature dependence, $R_\omega\sim T^{1.25}$ (for $r_p'=2.5$) and insertion of this into Eq. (10) yields $\sigma(\omega)\propto T^6$ for the uncorrelated case. This is obviously at variance with the much weaker temperature dependence exhibited by the low-temperature data of the present work (Fig. 5) and even if the correlated form[13] of the OLPT model is used, the dependence is predicted to decrease only to $\sigma(\omega)\propto T^4$. Thus the temperature dependence of the ac conductivity is not met in the framework of the OLPT model.

TABLE III. Parameters obtained from the OLPT model for various glass compositions at low temperatures.

Glass composition mol % V_2O_5	r_p'	W_{H0} (eV)	W_H[a] (eV)	r_p (Å)	α (Å^{-1})
70.8	3.0	0.61	0.338	1.63	0.92
75.6	2.5	0.57	0.326	1.55	0.82
80.5	2.0	0.53	0.317	1.43	0.73
85.5	1.6	0.52	0.310	1.42	0.59
90.3	1.4	0.50	0.301	1.40	0.56
95.2	1.4	0.48	0.288	1.39	0.52

[a]From Reference 5.

C. Correlated barrier hopping model

The correlated barrier hopping model [Eq. (15)] predicts that $\sigma(\omega)$ should behave, in some respects, in a similar manner to the OLPT model, namely, it should have a negative temperature dependence of the frequency exponent s and therefore it might be a possible contending theory for the ac conduction in the present vanadate system.

A critical test for the CBH model comes from the temperature dependence of the ac conductivity and its frequency exponent s. Fits to the experimental values of s as a function of temperature for one glass composition, made using Eq. (17), are shown in Fig. 4. The values of the parameters used in calculating the curves are those given in Table IV. A fixed frequency ($\omega=10^4$ s^{-1}) has been assumed for all glass compositions. From this figure, it is observed that the fit appears to be reasonable over a considerable temperature range. In Fig. 2(a), the measured total conductivity, $\sigma_{\rm tot}(\omega)$, is fitted to the measured values of the dc conductivity plus the ac conductivity calculated from Eq. (15) given by the CBH model, using W_M and τ_0 as variable parameters. The concentration of V^{4+} ions (Table I) is used for the values of N. The calculated curves are scaled so as to fit the value of $\sigma_{\rm tot}(\omega)$ at $\omega=2\pi\times10^5$ s^{-1} for the lowest temperature. The values of W_M and τ_0, obtained by the fitting procedure for various glass compositions, are collected in Table IV. The values of W_M are close to twice the value of high-temperature activation energy for dc conduction.[5] Similar results were also obtained from the simple HOB model for the tellurium vanadate system.[10] However, the values of τ_0 appear reasonably larger than those which would be expected for typical inverse phonon frequency.[5] Such a discrepancy is expected when the lattice relaxation effects are important[12] as we believe to be the case here.

D. Imaginary parts of the ac conductivity

Thus far, the real part of the ac conductivity [henceforth denoted by $\sigma_1(\omega)$] has been considered only neglecting the imaginary part [denoted by $\sigma_2(\omega)$] of the conductivity, which is related to the dielectric constant. Although the real and imaginary parts of the conductivity are related via the Kramers-Kronig relation, valuable information can be lost if $\sigma_2(\omega)$ is neglected. In particular, models for ac conduction also make specific predictions concerning the dielectric constant, and the comparison of theory and experiment is straightforward, since capacitance measurements are inherently much more accurate than conductance measurements when made using a conventional bridge technique.

The total measured capacitance $C_{\rm tot}(\omega)$, like the conductance, can be decomposed into two components, a dispersive term $C(\omega)$ and a nondispersive term C_∞, viz.

$$C_{\rm tot}(\omega)=C(\omega)+C_\infty \ . \tag{19}$$

These two components arise from different processes, C_α being due to high-frequency atomic and dipolar vibrational transitions, whereas $C(\omega)$ is determined by the loss mechanisms. Several methods[13] of eliminating the nondispersive component exist, e.g., measurements at high frequency, adjustment of C_∞ until the resulting $C(\omega)$ obeys a power-law dependence or numerical differentiation of the capacitance data whereupon the constant terms involving C_∞ drop out. Thus if the dispersive part of the capacitance obeys the power law

$$C(\omega)\propto\omega^{s'-1} \tag{20}$$

(where s' is not equal to s), a plot of $\log_{10}[-dc/d(\ln\omega)]$ versus $\log_{10}\omega$ should yield a straight line of slope $s'-1$. This differentiation technique has been used in the present work to determine $C(\omega)$. The ratio of the imaginary to the real part of the conductivity is then calculated from the relation

$$\sigma_2(\omega)/\sigma_1(\omega)=\omega C(\omega)/G(\omega) \ , \tag{21}$$

where $G(\omega)$ is the conductance at frequency ω.

It has been shown[13] that the quantity $\sigma_2(\omega)/\sigma_1(\omega)$ has a characteristically different functional form for the various mechanism of dielectric relaxation. Thus for the QMT model,

$$\sigma_2(\omega)/\sigma_1(\omega)=-(2/5\pi)\ln(\omega\tau_0) \ , \tag{22}$$

and for the CBH model, to a first approximation (for small k_BT/W_M)

TABLE IV. Parameters obtained by fitting with the CBH model for various glass compositions.

Glass composition mol % V_2O_5	τ_0 (s)	W_M (eV)	N (cm^{-3})
70.8	3×10^{-11}	0.70	7.69×10^{20}
75.6	5×10^{-11}	0.67	4.50×10^{20}
80.5	8×10^{-11}	0.64	4.21×10^{20}
85.5	2×10^{-10}	0.63	4.00×10^{20}
90.3	5×10^{-10}	0.61	3.96×10^{20}
95.2	6×10^{-10}	0.58	3.75×10^{20}

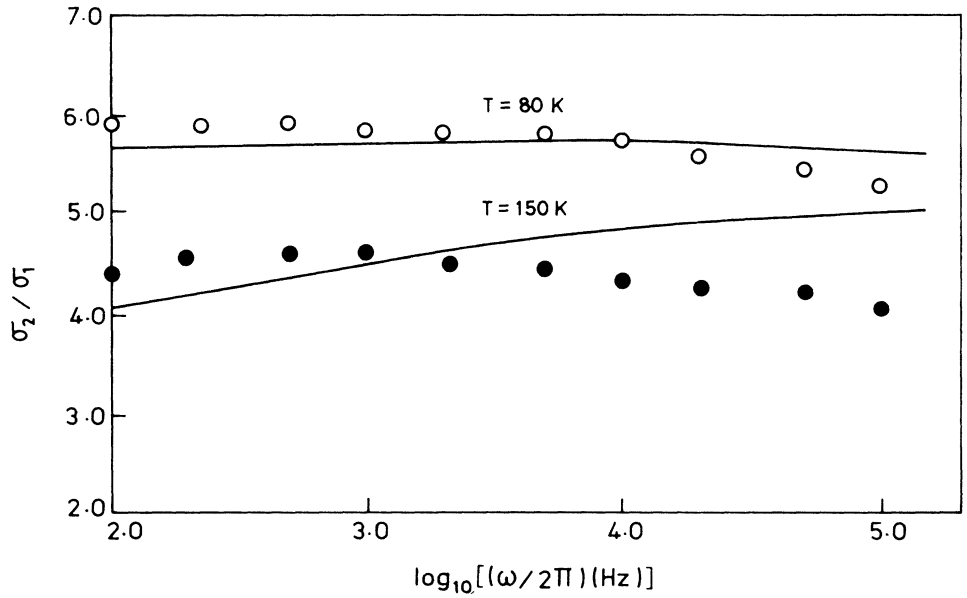

FIG. 7. Ratio of the imaginary and the real parts of the ac conductivity $[\sigma_2(\omega)/\sigma_1(\omega)=\omega C(\omega)/G(\omega)]$ for the sample composition $80(V_2O_5)$-$20(Bi_2O_3)$ at two temperatures shown. The solid curves represent the behavior of $\sigma_2(\omega)/\sigma_1(\omega)$ predicted by the CBH model [Eq. (23)].

$$\sigma_2(\omega)/\sigma_1(\omega) = -(2/\pi)\ln(\omega\tau_0)[1+(3k_BT/W_M)\ln(\omega\tau_0)] . \quad (23)$$

It may be noted that Eq. (23) predicts a temperature dependence for $\sigma_2(\omega)/\sigma_1(\omega)$, whereas Eq. (22) does not. For the OLPT model, $\sigma_2(\omega)/\sigma_1(\omega)$ behaves like that for the simple QMT model at high temperatures, whereas at low temperatures the behavior is similar to that exhibited by the CBH model.

In Fig. 7 the experimental data for $\sigma_2(\omega)/\sigma_1(\omega)$ [calculated from Eq. (21)] are plotted versus $\log_{10}\omega$ for one glass composition at two temperatures. It is observed that $\sigma_2(\omega)/\sigma_1(\omega)$ is temperature dependent which implies the simple QMT model is not applicable. Also shown in the figure are the curves corresponding to the prediction of the CBH model [Eq. (23)], drawn using the same values of the parameters W_M and τ_0 (Table IV) already deduced from the fitting of the real part of the conductivity to the CBH model. The fit between theory and experiment may be regarded as good, bearing in mind that no extra variable parameters are used in the calculation of $\sigma_2(\omega)/\sigma_1(\omega)$ from Eq. (23). The qualitative behavior of the frequency and temperature dependence of $\sigma_2(\omega)/\sigma_1(\omega)$ is reproduced by the CBH model and the magnitude is correct to within 10%. The discrepancy is ascribed to the fact that Eq. (23) is only approximate; higher-order terms become important at high temperatures. It should be noted that the fits to $\sigma_2(\omega)/\sigma_1(\omega)$ are very sensitive to the values of the parameters used (e.g., τ_0 and W_M) and are more sensitive than the fits made to just the real part of the ac conductivity.

VI. CONCLUSIONS

The real and imaginary parts of the frequency-dependent (ac) conductivity of the bismuth-vanadate glassy semiconductors have been presented, for the first time, in the frequency range 10^2-10^5 Hz and in the temperature range 77–420 K. Analysis of the ac data in the light of the various theoretical models (described in Sec. II) shows that the CBH model is the most appropriate for explaining quantitatively the frequency and temperature dependence of the ac conductivity and its frequency exponent. The parameters obtained by fitting the experimental data to this model appear reasonable. Although the QMT model fails to predict the temperature dependence of the frequency exponent, it is consistent with the temperature dependence of the ac conductivity at low temperatures. The temperature dependence of the frequency exponent is in agreement with the OLPT model at least in the low-temperature range. The OLPT model yields reasonable values of the decay constant. However, this model predicts temperature dependence of the ac conductivity which is much stronger than the experimental data showed.

ACKNOWLEDGMENTS

The author is highly grateful to Professor U. S. Ghosh, Head of the Department of Solid State Physics, for his interest in this work. He also wishes to thank Professor A. Mansingh, Department of Physics and Astrophysics, University of Delhi for his various suggestions.

[1]N. F. Mott, J. Non-Cryst. Solids **1**, 1 (1968).
[2]I. G. Austin and N. F. Mott, Adv. Phys. **18**, 41 (1969).
[3]M. Sayer and A. Mansingh, Phys. Rev. B **6**, 4629 (1972).
[4]C. H. Chung and J. D. Mackenzie, J. Non-Cryst. Solids **42**, 151 (1980).
[5]A. Ghosh and B. K. Chaudhuri, J. Non-Cryst. Solids **83**, 151 (1986).
[6]A. E. Owen, J. Non-Cryst. Solids **25**, 370 (1977).
[7]L. Murawski, Philos. Mag. B **50**, L69 (1984).
[8]A. Mansingh, R. P. Tandon, and J. K. Valid, Phys. Rev. B **21**, 4829 (1980).
[9]A. Mansingh, J. K. Valid, and R. T. Tandon, J. Phys. C **8**, 1023 (1975).
[10]A. Mansingh and V. K. Dhawan, J. Phys. C **16**, 1675 (1983).
[11]N. F. Mott and E. A. Davis, *Electronic Processes in Non-Crystalline Materials,* 2nd ed. (Clarendon Press, Oxford, 1979).
[12]S. R. Elliott, Adv. Phys. **36**, 135 (1987).
[13]A. R. Long, Adv. Phys. **31**, 553 (1982).
[14]M. Pollak, Philos. Mag. **23**, 519 (1971).
[15]H. Bottger and V. V. Bryskin, Phys. Status Solidi B **78**, 415 (1976).
[16]P. N. Butcher and K. J. Hayden, in *Proceedings of the 7th International Conference on Amorphous and Liquid Semiconductors,* edited by W. E. Spear (Centre for Industrial Consultancy and Liaison, University of Edinburgh, Edinburgh, 1977), p. 234.
[17]A. L. Efros, Philos. Mag. B **43**, 829 (1981).
[18]M. Pollak, Phys. Rev. **138**, A1822 (1965).
[19]M. Pollak and G. E. Pike, Phys. Rev. Lett. **28**, 1449 (1972).
[20]G. Frossati, R. Maynard, R. Rummal, and D. Thoulouse, J. Phys. (Paris) Lett. **38**, L15 (1977).
[21]G. E. Pike, Phys. Rev. B **6**, 1572 (1972).
[22]S. R. Elliott, Philos. Mag. **36**, 1291 (1977).
[23]S. R. Elliott, Philos. Mag. B **37**, 553 (1978).
[24]S. R. Elliott, Philos. Mag. B **40**, 507 (1979); J. Non-Cryst. Solids **35-36**, 855 (1980).
[25]I. G. Austin and E. S. Garbett, in *Electronic and Structural Properties of Amorphous Semiconductors,* edited by P. G. Le Comber and J. Mort (Academic, London, 1973), p. 393.